Topological theory of electron-phonon interactions in high-temperature superconductors

J. C. Phillips
Department of Physics and Astronomy, Rutgers University, Piscataway, New Jersey 08854-8019, USA
(Received 9 September 2004; revised manuscript received 7 December 2004; published 12 May 2005)

There are large isotope effects in the phonon kinks observed in angle-resolved photoemission spectroscopy of optimally doped cuprate high-temperature superconductors (HTSC), but they are quite different from those expected for a nearly free-electron metal (Fermi *liquid*) with strong electron-phonon interactions (Eliashberg model). These differences, together with many other anomalies in infrared spectra, seem to suggest that other particles (such as magnons) must be contributing to HTSC. Here we use topological methods to discuss the data, emphasizing nanoscale phase separation and the importance of a narrow band of quantum *percolative* states near the Fermi energy that is spatially pinned to a *self-organized* filamentary dopant array, resulting in a filamentary *glass*. Topological discrete, noncontinuum, nonperturbative methods have previously explained the form of HTSC phase diagrams without involving detailed microscopic assumptions, and they are especially useful in the presence of strong nanoscale glassy disorder. These methods also explain the "miracle" of an ideal nearly free-electron (gas or liquid) phonon kink in sharply defined nodal quasiparticle states in LSCO at the metal-insulator transition. Careful study of the data reveals anharmonic phonon interactions. Finally, the universality of the kink energy and Fermi velocities below the Debye cutoff in different cuprates is the result of the marginally elastic nature of these configurationally glassy materials, and specifically the isostatic character of the CuO_2 planes.

DOI: 10.1103/PhysRevB.71.184505 PACS number(s): 74.72.−h

I. INTRODUCTION

Since the discovery of high-temperature superconductivity in the cuprates,[1] the foremost question in physics has been what are the interactions responsible for this completely unexpected phenomenon. Mueller himself has always argued that they must be strong electron-phonon interactions, and it was the expectation that these interactions would be strong in generically unstable perovskitelike materials that led to his experiments on doped cuprates, carried out contrary to the received wisdom that superconductivity would be suppressed by antiferromagnetic interactions. However, the isotope effects on T_c that were the signature of strong electron-phonon interactions in metals have behaved perversely in the ceramic cuprates, being large, as in metals, near the metal-insulator transition and becoming small near optimal doping. Indeed the search for isotope effects in the cuprates directly related to superconductivity has seldom been successful.[2] Such elusive behavior suggested that some other interaction might be involved, but what could this be? Magnons have often been suggested, but these are unreasonable: (i) although it might seem that exchange of any boson can generate Cooper pairs, magnon scattering also destroys Cooper pairs, in other words, magnons suppress, not enhance, superconductivity, as is evident from phase diagrams, where increasing dopant density initially quenches magnetic phases, before the superconductive phase is reached; (ii) electron-magnon coupling is smaller than electron-phonon coupling (spin-orbit coupling constants for Cu and O are of order 10^{-2} eV or less, compared to phonon energies of order 10^{-1} eV, and (iii) beyond the metal-insulator transition, when T_c is growing toward optimal doping, the filling factor for magnons is decreasing rapidly. Ignoring these reasons, many theorists have continued to use magnons and/or spins to explain various angle-resolved photoemission spectroscopy (ARPES) and infrared anomalies, especially in underdoped samples, but here these anomalies will be explained topologically, with magnons playing only a very minor role.

The disappearance[3] of isotope shifts in T_c near optimal doping could be the result of the optimization process itself:[3] small isotope effects "are expected when vibrational frequency changes are compensated by internal coordinate changes." Here we will show that these apparently complex and immeasurable configurational changes are associated with dopant coordinates and that the latter are nearly perfectly self-organized.[4] This explains quite simply and very accurately the central anomalies in the large isotope shifts recently observed[5] near optimal doping in $Bi_2Sr_2CaCu_2O_{8+\delta}$ (BSCCO) by ARPES.

Some cautionary remarks are appropriate here. Together with analysis, geometry, and algebra (including group theory), topology is one of the established fields of modern mathematics; it is also the youngest. Although there are some papers in theoretical physics that adopt a topological approach, this style is unfamiliar to most physicists. Topological techniques are used here for treating the problems of strong glassy disorder that arise from the pinning of current carriers to dopants and the associated percolative conduction processes in both the normal and superconductive states of high-temperature superconductors (HTSC). Conventional (nonpercolative) effective medium (single-phase) theories of the metal-insulator transition predict only a *single* transition, but in the cuprates as the dopant density increases, there are *two* transitions: first, from the semiconductive phase to the intermediate or "strange metal" percolative superconductive phase, and second, from intermediate phase to the normal metal (nonsuperconductive Fermi-liquid) phase. These topological methods have previously been used to explain the origin of the percolative intermediate phase associated with HTSC and why it has many anomalous properties,[6] as well

as why this phase occurs *chiefly in cuprates* and seldom in the thousands of other perovskitelike oxides.

Readers who are unfamiliar with the constraint theory of network glasses (1980s–present) will also find that the present paper contains many different and difficult ideas. This is unavoidable because the properties of the cuprates are very, very different from those of normal metals, so that any realistic theory will not resemble any already well-known general model [such as the Sommerfeld nearly free-electron *gas* model of simple metals (1920s) or its Landau quasiparticle (Fermi-*liquid*) refinements (1950s) or the Hubbard model (1960s), so widely misapplied to the cuprates]. This paper takes the reader beyond simple (1920s–1960s) models in two stages: first, to a percolative model, and then to a *specific kind* of percolative model, namely, the filamentary *glass* model in which the percolative paths have been optimized (self-organized) in ways discussed below that are characteristic of ideal network glasses, both electronic and molecular.

II. THE PHOTOEMISSION KINK

A dispersive kink (discontinuous change in slope) in $E(\boldsymbol{k})$ for $\boldsymbol{k}$ along (11) in the *ab* plane appears[7] in ARPES spectra for (Pb-doped)BSCCO and LSCO. The energy E_k ($\sim$70 meV) at which the change in slope occurs is somewhat above that of the zone-boundary LO phonon known[8,9] to be correlated with HTSC, but unambiguously different from magnon energies ($\sim$40 meV). The large isotope shifts[5] decisively support the phonon interpretation of the dispersive kink, but they raise new problems.

In a conventional Sommerfeld gas or Landau-liquid model[10] dominated by a single Einstein LO phonon mode, coupled to a Fermi liquid with an electron-phonon coupling constant λ, and self-consistently broadened by many-phonon decay effects,[11] the phonon contribution to the quasiparticle self-energy inferred from momentum distribution curves (MDC) increases linearly with $|\boldsymbol{k}-\boldsymbol{k}_F|$ up to the phonon cutoff energy Θ_D and then vanishes. (If instead energy distribution curves are used, then the phonon contributions below and above Θ_D are both nearly linear, but of opposite sign, and near the phonon energy there are two "noncrossing" branches to the dispersion curve.) In the absence of many-phonon decay effects the MDC inverse dispersive slope $m^*_< = m^*_0/(1+\lambda)$ up to the phonon cutoff energy Θ_D, and then is unchanged, $m^*_> = m^*_0$. With many-phonon decay effects in both cases the changes in m^* on crossing Θ_D are reduced by a factor of about 3 for $\lambda = 1.5$ compared to the unbroadened value of slope changes. In this Fermi-liquid (Eliashberg) model[11] the measured MDC dispersion line should be pinned to the bare dispersion line for $|E-E_F| > \Theta_D$ and for $E=E_F$, so that there is a discontinuity δE at $|E-E_F| = \Theta_D$ (see Fig. 1).

Experimentally[5] (see Fig. 2) near optimal doping the situation is exactly *reversed*: the isotope shifts for both energy and momentum distributions are *nearly zero* up to the kink energy E_k, which is also the phonon cutoff energy Θ_D, so that $m^*_< \equiv m^*_0$. Then they begin to increase linearly with $E-E_k$. ($m^*_> \neq m^*_<$), without a discontinuity ($\delta E = 0$). This

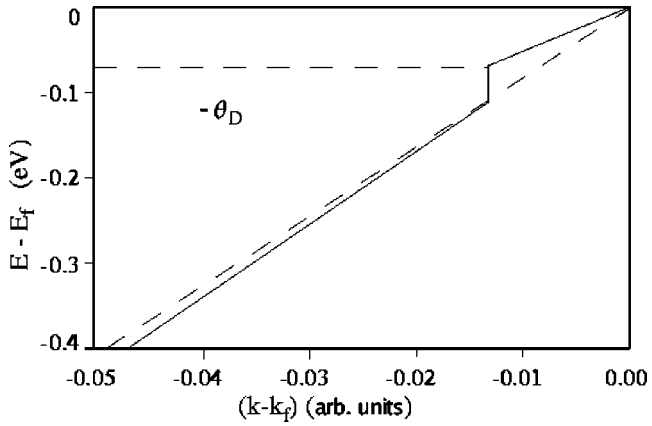

FIG. 1. The "ideal" quasiparticle dispersion of a Fermi-Landau liquid interacting with an Einstein phonon of energy Θ_D, measured in photoemission from momentum-distribution curves (see Fig. 5 of Ref. 11). The dashed line shows the bare dispersion curve without phonons, and the position of the Einstein phonon energy is marked.

nearly perfect cancellation below Θ_D echoes the cancellation at optimal doping of the isotope shift in T_c itself. Additionally, the large isotope effects above Θ_D continue right up to the point that the signal is incoherently broadened, a seemingly uncontrolled increase that is rarely encountered (a lower cutoff without an upper one).

In addition to this cancellation below Θ_D, the relative isotope shifts above Θ_D *change sign* as $\boldsymbol{k}$ moves from the nodal gap direction (11) toward the antinodal direction (01). In both directions the slope increases above Θ_D [$(m^*_>/m^*_0) < 1$]; in the nodal direction (Ref. 5, Fig. 2, curve 1) the increase is larger for ^{18}O than for ^{16}O ($^{18}m^*_> < {}^{16}m^*_>$), whereas the reverse holds as $\boldsymbol{k}$ moves closer to the antinodal direction (Ref. 5, Fig. 2(a), curve 6). Moreover, the isotope shift has the same anisotropy as the energy gap, leading to a linear relation between the two [inset, Ref. 5, Fig. 2(a)]. The increase in slope above Θ_D means that the effective mass m^* has decreased; in Fermi-liquid models[7] this is interpreted as an undressing of $m^*_< = m(1+\lambda)$ below Θ_D to $m^*_> = m$ above Θ_D. Ordinarily one would expect a larger effect for heavier

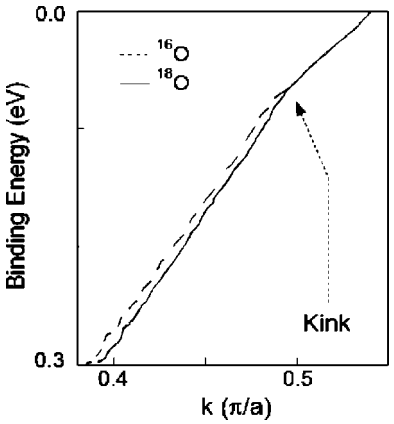

FIG. 2. Isotope-induced changes of the nodal dispersion measured by ARPES in BSCCO near optimal doping (after Fig. 1 of Ref. 5).

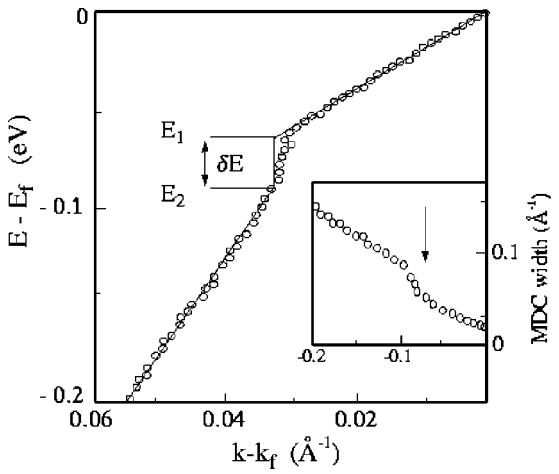

FIG. 3. "Ideal" dispersion in the nodal direction in $La_{2-x}Sr_xCuO_4$ at $x=0.063$ (insulator-metal transition) (after Fig. 1(b) of Ref. 14). Here $E_1 \sim -0.06$ meV and $E_2 \sim -0.09$ meV. These two energies correspond respectively to the bottom of the optical phonon band and the infrared cutoff (Refs. 33 and 34).

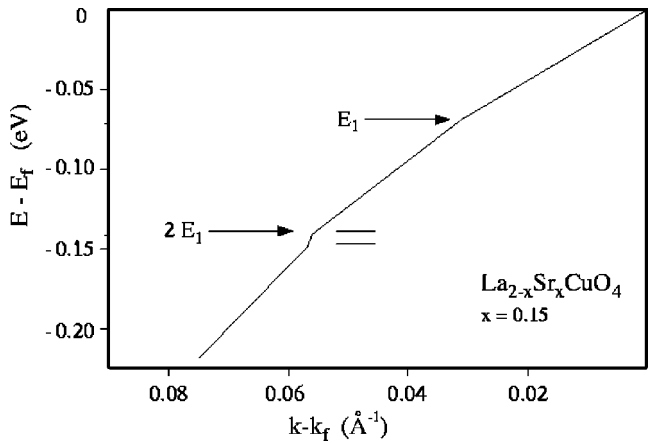

FIG. 4. Dispersion in the nodal direction in $La_{2-x}Sr_xCuO_4$ at $x=0.15$ (optimal doping) (after Fig. 1(a) of Ref. 13). These preliminary data suggest that there are two kinks in the dispersion curve, corresponding to one- (E_1) and two-phonon ($2E_1$) cutoffs; there may even be a discontinuity at the latter. The crowding effects of filaments near optimal doping that are illustrated in Fig. 5, or simply increasing dopant-driven lattice instabilities,[40] could cause the increased strength of the two-phonon interactions, but the most attractive explanation is the "knot" mechanism mentioned in the text. (The theory of knots is a separate subject of topology, quite complex in $d>2$ dimensions. Here we have only the case $d=2$, and the only possible knot is that formed by the intersection of two strings or filaments.)

masses (normal isotope effect, $\lambda \sim M^{-\alpha}$, with $\alpha \sim 1/2$), as observed in the antinodal direction. However, off-lattice configurational instabilities can produce inverse isotope effects, for instance, with interstitial H in Pd because of zero-point motion.[12] In this case one expects the relaxing carriers to move towards E_F. Thus the behavior of the antinodal direction (strong electron-phonon interactions) is "normal," whereas in the nodal direction it is "inverse," indicative of compensating configurational relaxation.

What is the reason for the disappearance (Fig. 2) of the discontinuity δE in the dispersion line predicted by quasiparticle models (Fig. 1)? As we shall see, this is the consequence of self-organized correlation of multiple percolative nonmomentum conserving paths near *glassy* optimal doping. However, before we proceed to discuss this complex phenomenon, we can note that, in fact, the theoretically predicted Fermi-liquid discontinuity δE has been observed[13,14] in ARPES spectra along the nodal direction in the low-density limit near and below the metal-insulator transition in $La_{2-x}Sr_xCuO_4$ at $x=x_c=0.063$ [their Fig. 1(b), shown here as Fig. 3], described by the authors as "a miracle." For dopant densities near and below the metal-insulator transition there are only a few percolative paths (or path segments), and interactions between carriers on different paths can be neglected. Carriers move freely along these paths, unhindered by constraints imposed by interpath interactions, and can thus be described by the usual momentum-conserving quasiparticle formalism. From the limited published data it appears that the discontinuity δE decreases with increasing x and either disappears or broadens (Fig. 4) near optimal doping at $x=x_o \sim 0.16$.

For the reader's convenience the foregoing discussion is summarized compactly in Table I. If one accepts the predictions of Fermi-liquid theory as natural or "intuitive," then the table shows that *all* the experimental results are "counterintuitive."

III. NANOSCALE PHASE SEPARATION AND THE PARTICIPATION RATIO

Scanning tunneling microscopy (STM) has produced[15,16] quantitative pictures of nanodomain structures on very carefully cleaved (in situ at low T) micaceous BSCCO. The I-V traces are spatially reproducible on a length scale of 0.15 nm and time scale of weeks, permitting unprecedented surveys of nanodomain and impurity electronic structures. The single most striking aspect of the early data was the near constancy of the nanodomain diameter at 3 nm, independent of doping within the superconductive phase, suggestive of ferroelastic interactions with cutoffs on stress accumulation, consistent with theoretical expectations based on the general properties of perovskites and related ceramics.[17,18] (Again, it was the expectation of strong electron-phonon interactions in ferroelastic pseudoperovskites that guided Bednorz and Mueller in their original work.) Subsequent scans have revealed an excellent checkerboard gap structure[16,19] of alternating superconductive ($\sim$40 meV) and pseudogap ($\sim$60 meV) 3 nm domains over a field of view of 65 nm^2 ($\sim$40,000 unit cells) near optimal doping. Fourier transforms of the underdoped two-gap structure have shown that there is a charge-density wave (CDW) associated entirely with the larger pseudogap ($>$60 meV) majority nanodomains, whereas the lattice structure associated with the smaller superconductive gap pockets ($<$60 meV) is undeformed.[20] This kind of structural pattern is readily explained in terms, for example, of orthorhombic stress patterns that are frustrated and leave behind small residual unstressed pockets near larger nanodomain corners.

Fourier transforms of "octet" subgap states reveal "*d*-wave symmetry" gap anisotropy proportional to $|\cos 2\phi|$. What is most remarkable about the anisotropy is that in ARPES and also STM data, it holds for the superconducting gap within a few percent for optimally and overdoped samples.[19] It is important to note that the *d*-wave gap *projected in this way as an order parameter* represents only a small fraction (probably $<10\%$) of the subgap states and that the latter are merely a tail on the superconductive density of states itself. Almost all the states responsible for HTSC are not included in the Fourier projection, which means that they are not indexable by $\boldsymbol{k}$ and are not describable by *d* waves. The Fourier transforms *project* gap order on plane waves, much as participation ratios attempt to identify delocalized states in simulation models of metal-insulator transitions. Note that a fraction as small as 10% is inexplicable for a metallic participation ratio in models containing random disorder, and it cannot be explained merely as a result of fluctuations in two dimensions because of Coulomb interactions,[21] even if the on-site Coulomb interactions U are 50 times larger than the bandwidth W. In view of the easily deformed nature of perovskites and pseudoperovskites, a much more plausible, material-specific explanation for the observed structure (including charge-density waves) is provided by the self-organized internal stress patterns discussed above, and elaborated in considerable detail elsewhere.[18,22] An important point here is that projecting Cooper pair amplitudes on percolative paths provides a *rigorous derivation*[22] of the *d*-wave gap anisotropy proportional to $|\cos 2\phi|$. The factor 2 arises from Cooper pairing.

IV. DOPANT SELF-ORGANIZATION AND NARROW COHERENT PERCOLATIVE FERMI ENERGY BAND

Conventional percolation theory is inconsistent with the small fraction of percolating gap states. In Fermi systems one can suppose[23,24] that there is a narrow energy band of coherent percolative states centered on self-organized dopant configurations [filaments, not stripes (a misnomer) because in the superconductive regions the dopants are disordered and do not form a superlatttice]. The dopants are not randomly distributed, as in conventional percolation theory, but form an internal template for microcircuitry. The dopants organize to form filaments ("pearls on a string") because such filaments, with their high conductivities, minimize the free energy by maximizing the enthalpy gained from screening of internal electric fields ("anti-Jahn-Teller-effect").[25] The filaments are three-dimensional,[23] zigzagging coherently through dopants (located outside the CuO_2 planes) to avoid insulating nanodomain walls in metallic planes: this explains why in high-quality samples *c*-axis conductivities and London carrier densities follow the same coherent scaling relations,[26] extended to much smaller values, as those in the *ab* plane. This scaling relation covers more than six decades and includes Nb and Pb (Fermi-liquid metals) for high carrier densities. We can note that without a percolative model, the *c*-axis conductivity could not be coherent; it would have to arise from carrier hopping.

Self-organized configurations cannot be identified by algebraic methods applied to continuum Hamiltonians, but their properties are known in several other ways. The combinatorial problems that arise in attempting to identify such optimized percolative paths are exponentially difficult (or as mathematicians say, NP complete). Self-organization in strongly disordered media was discussed in the context of the intermediate phase in network glasses,[6,27] and it has since been analyzed in numerical simulations of steadily increasing sophistication.[28–30] (The most recent effort[30] involves 40,000 atoms.) The glassy, strongly disordered nature of the intermediate superconductive phase contrasts with narrow infrared, Raman and neutron linewidths[31] in the crystalline superlattice 1/8 "stripe" phase (superconductivity suppressed) of LSCO; thus these widths are much wider at optimal doping, and percolative filaments should *never* be confused with crystalline stripes. Such a narrow percolative energy band has often been proposed: a recent example utilized sum rules for the infrared conductivity.[32] The difference $W_n - W_s$ of the integrated planar real part of the conductivity above and below T_c extends to high energies ($\sim$3000–4000 cm^{-1}) in BSCCO or LSCO because of strong (polaronic) LO phonon interactions at dopants.[33,34]

A characteristic feature of this percolative band is its zigzag character: in the *ab* plane it consists of line segments parallel to Cu-O bonds.[35] The (10) antinodal superconductive states centered on dopant arrays thus have a "strong forward-scattering" character when treated by nearly free-electron *gas* scattering theory.[36] Suppose that filamentary formation is enhanced by decreasing the ratio $r = t'/t$ of second-neighbor (11) overlap to nearest-neighbor (10) Cu-O overlap in the CuO_2 plane and that such topological enhancement increases T_c. Abrecht *et al.* observed a reduction in r of a factor of 6 in severely compressed overdoped LSCO films,[37] accompanied by a large decrease in $N(E_F)$. According to continuum mod-

TABLE I. Comparison of predictions of effects of electron-phonon interactions on effective masses below ($m^*_<$) and above ($m^*_>$) the Debye energy Θ_D in theoretical liquid and glass models with ARPES experiments. (The Hubbard model can be regarded as a Fermi hard-sphere lattice gas.) The subscripts *n* and *an* refer to nodal (11) and antinodal (10) electron planar momentum orientations, respectively, m_0^* is the bare mass, $a, \ldots, d$ are constants with $a<b$ and $c<d$, x is the Sr dopant concentration in $La_{2-x}Sr_xCuO_4$ (LSCO), and $c'(x) \sim 2 > 0$. The BSCCO data are taken near optimal doping and refer to the isotope shift (δ) caused by replacing ^{16}O with ^{18}O. Thus (for example) $\delta m^*_<$ (BSCCO) = 0 (no change), $\delta m^*_{>_n}$ (BSCCO) < 0. There is no simple connection between the isotope shift δm^* and the isotope shift δT_c. However, broadly speaking, δT_c is large when $m^*_</m_0^* > 1$ (see Sec. V and Ref. 38 for discussion of the gap equation that determines δT_c).

Model	$m^*_</m_0^*$	$(m^*_>/m_0^*)_n$	$(m^*_>/m_0^*)_{an}$	Ref.
Fermi liquid	$1+\lambda$	1	1	10,11
Mean-field Hubbard	1	1	1	54
Dopant glass $[c<d]$ (δ)	1	$[c-(\varepsilon)]<1$	$[d+(\varepsilon)]>1$	Here
Experiment (BSCCO) (δ)	1	$[a-(\varepsilon)]<1$	$[b+(\varepsilon)]>1$	5
Experiment (LSCO)	1	$c(x)<1$		13

els, the decrease in $N(E_F)$ should have reduced T_c. In fact, T_c actually increased to a value higher than is found in unstrained optimally doped LSCO, proving that in cuprates topological factors that favor filamentary formation are more important than continuum factors, such as $N(E_F)$, in determining T_c.

V. TOPOLOGICAL THEORY

With these elements in place, one can discuss the first problem, why at optimal doping $\delta E=0$ and the isotope shifts are small both for T_c and for $m^*_<$, the dispersive $E(\boldsymbol{k})$ *below* the phonon cutoff energy Θ_D. Of course, the attractive well in the gap equation[38] lies below Θ_D so the ARPES observation of small isotope shifts below Θ_D at optimal doping is equivalent to small isotope shifts for T_c. But why are the ARPES shifts at optimal doping so small below Θ_D?

Constraint theory is a generic theory for dealing with strongly disordered, but still self-organized, systems (electronic and molecular glasses).[35] It has explained many of the properties of network glasses (stiffness transitions, phase diagrams, including reversibility windows,[27] for ~10 different binary and ternary chalcogenide alloys, and even the nearly ideal properties of Si/SiO_2 interfaces[39]). These ideas also explain the marginal elastic stability of cuprates, which explains[40] why they are the only HTSC. Broadly speaking, Lagrangian constraint theory is a hierarchical topological theory that relies on the existence of groupings of interatomic or electronic potentials in selected materials—for instance, bond-stretching and bond-bending interactions in network glasses. It is effective for only a small class of ideally disordered solids where intact constraints have frozen a liquid into a glass and obstructed crystallization. However, that class contains exactly those glassy materials, including cuprates, which have posed the hardest problems for conventional algebraic and/or analytical theories. Indeed, topology (including set theory) emerged as a separate branch of mathematics when mathematicians realized (a little more than 100 years ago) that there exists a class of exponentially complex problems that are insoluble by other methods. Here we hope to develop the general topological approach in the context of the rich experimental literature that has recently emerged for the cuprates.

The central idea of constraint theory is that in a fully self-organized ideal network strong disorder causes the strongest constraints to be almost perfectly intact, whereas the weaker ones are absolutely broken.[6,41] [Intact (broken) molecular constraints are easily recognized as sharp (broad) peaks in radial distribution functions, or from narrow (broad) Raman bands. In molecular glasses the weakest intact constraining bonds are typically three times stronger than the strongest soft constraining bonds; in other words, there is a Lagrangian gap in the bond-strength spectrum between intact and broken constraints. The existence of this Lagrangian gap is crucial to glass formation.] In algebraic language, the condition $N_c \equiv N_d$, where N_c is the number of intact constraints, and N_d is the number of degrees of freedom, is *exact* in an ideal glass. (Here and later $\equiv$ means identical within polynomial accuracy. There may still be corrections that are exponentially small associated with network defects; examples will be given. In practice these exponentially small corrections are often not observable, and so far they have not been observed by ARPES in m^*.)

In molecular glasses one observes close parallels between the composition dependence (phase diagrams) of two quantities. The first quantity is the slope of the viscosity η of the supercooled *liquid* as $T \to T_g$, $(d \log \eta / dT)_{Tg}$, which has commonly been used by chemists to measure the "strength" of a glass, as this quantity is largest for network glasses and decreases in molecular and polymeric glasses. (The viscosity is a direct measure of the residual free-particle nature of the glass-forming supercooled liquid.) The second quantity is the irreversible part of the enthalpy ("memory") of the glass transition, which is smallest when constraints are sharply defined. This correlation shows that there is a direct connection between the transport properties of glass-forming liquids and the countable number of shortest range bonding constraints in the glass; the latter are partially intact in the supercooled liquid as well, affecting mobilities in a precursive way. (Broadly speaking, this is the reason why so many precursive effects have been observed in the cuprates.) The number of strongest atomic constraints N_c is *always* limited by the discrete number of atomic degrees of freedom N_d of the glass, an idea[41,42] whose applications have multiplied vigorously in the last 25 years, as illustrated in a recent popularized presentation of the theory.[43]

Here we are concerned with self-organization of a Fermionic system in the presence of long-range Coulomb and strain interactions. Because of the Fermi exclusion principle, hierarchical interactions constrain glassy electronic configurations differently from those in glassy molecular systems driven by classical interatomic forces. In the case of molecular glasses, the constrained interactions are the strongest ones and counting them is a straightforward application of Pauling's theory of resonating bonds. In Fermi systems the most constrained carriers are the most weakly bound (highest energy) ones nearest the Fermi energy. This paradoxical result is caused by the fact that (because of the exclusion principle) the largest carrier energy can be gained from long-range Coulomb and strain interactions by polarizing the carriers nearest the Fermi energy.

Of course, in strongly ionic ceramics, such as the cuprates, the phonons that embody long-range Coulomb and strain interactions best are longitudinal-optic (LO) phonons. In materials with partially ionic bonds similar to the cuprates, such as ZnO, the 3.4 eV luminescence phonon sidebands associated with LO phonons are typically 5–10 times stronger than those associated with other phonons;[44] thus, only LO phonon interactions are able to constrain carrier motion. (Recall that in molecular glasses, as discussed above, the Lagrangian hierarchical gap between broken and intact constraints is typically a factor of 3.) In the doped cuprates there are localized LO phonons that bind to carriers associated with dopants to form polarons resonantly bound to dopants. These states are different from conventional free polarons and have distinctively glassy properties. They could be called dopolarons to emphasize this point.

Because the cuprate host lattice is so ionic, the strongest forces are Coulombic and the strongest electronic constraints

are those associated with the most polarizable states, which are those nearest E_F. All the carriers within Θ_D of E_F can form (do)polarons by taking advantage of the interaction with an equal number of LO phonons localized near the same number of dopants, with polarization vectors parallel to the local filamentary tangent (the filament need not be linear, and the dopants need not be spaced periodically, as in a commensurate stripe). Once again $N_c \equiv N_d$, and this condition is *polynomially exact*. Although in the molecular cases one must rely on the extensive structural and spectroscopic data available for chalcogenide and oxide network glasses, counting constraints for dopolarons is so simple that one is justified in describing the procedure as trivial. This kind of result—something apparently profound and inaccessible is obtained after some discussion by a very simple and straightforward calculation—is typical of topology.

The electric dipole oscillator strengths of such coherent filamentary dopolarons are far larger than those of any incidental localized states that may coexist elsewhere in the sample (for example, in the exponentially small tails of pseudogaps in magnetic or charge-density wave nanodomains.) Thus the excitations of coherent filamentary states dominate optical spectra (infrared or ultraviolet) involving excitation of states belowΘ_D. (Speaking figuratively, the dopolarons are like shining pearls on strings.) The *integral* number of such LO phonons is assumed to be one per (electrically active) dopant, so the number of constrained carriers below the Debye energy matches the number of dopants *exactly*, for all dopant densities, and are unaffected by isotope exchange, below strongly overdoped, where the (nonglassy) normal Fermi-liquid state forms. (In other words, bound (or "impurity") dopolarons are counted relative to the glassy dopant array and not relative to the crystalline host atoms, which merely form a background medium.)

Of course, this constraint matching condition $N_c \equiv N_d$ is independent of the dopant density (so long as we are in the intermediate phase,[30] which is neither insulating nor normal metallic), in agreement with experiment,[13] which shows $m^*_<$ to be independent of the dopant density (to within$\sim$10%). This is a success of constraint theory; it is not merely qualitative or quantitative, in the glassy context it is exact. At the same time, $m^*_>$ varies rapidly with dopant density, which is to be expected, as the constraints that stabilize the most polarizable states of the dopant array with $|E-E_F|<\Theta_D$ are exhausted at $|E-E_F|=\Theta_D$. For $|E-E_F|>\Theta_D$ the marginal stability of perovskitelike host lattices leads to large shear instabilities near dopants. These, in turn, increase the dopant polarizability. The value of $m^*_>$ increases[13] by a factor of $1/2$ (the apparent bandwidth decreases by a factor of $1/3$) as the super-Debye carriers are pinned to dopants on going from $x=0.03$ to $x=0.30$ in $La_{2-x}Sr_xCuO_4$., corresponding to $dm^*_>/dx \sim 2$. This is another success of constraint theory. The 33% change in bandwidth could not occur in any conventional mean-field model of electronic interactions in a stable lattice, as the average valence N_v of a $La_{1-x}Sr_xO_{(3-x)/2}$ unit has changed by only 6% ($dN_v/dx=0.5$). The small changes in $m^*_<$ are consistent with the small changes in N_v, while the large changes observed in $m^*_>$ or bandwidth must be caused by dopant-related lattice instabilities, a kind of local-field, dopant-driven dielectric mechanical catastrophe. Similar (but much weaker) instabilities have been observed[45] in metallic superconductors, such as NbN and V_3Si.

The second problem, the anisotropy of the shifts for dispersive energies more than Θ_D away from E_F, is more difficult. The "normal" isotope shift (states with larger masses $m^*_>$ shifting more toward E_F, in other words relaxation enhances the polarizability) is what we would expect from filamentary states bound to dopants as they relax to improve dielectric screening of the dopant potentials (the previously identified "anti-Jahn-Teller effect"):[25] these states are obviously antinodal states. The nodal states, on the other hand, must be orthogonal to the antinodal filamentary states. (Recall here that ARPES measures only projections of actual disordered states, but orthogonality is still present after the projection.) Then phase-space incompressibility dictates that as the larger mass antinodal states reorder to move closer to E_F, the more weakly interacting nodal states should reorder to move away ("inverse" isotope shift). The two shifts approximately cancel, leaving little or no net isotope effect near optimal doping in the angular average $m^*_>$ even above the phonon cutoff energy Θ_D, where one expects Fermi-Landau theory[11] to be valid. In the Cooper pair channel, the net primary interaction above the phonon cutoff energy Θ_D is still Coulomb repulsion (just as in metals), whereas below the phonon cutoff energy Θ_D it is still attractive electron-phonon interactions, with an isotope effect concealed by the self-organized glassiness of the dopant configurations.

In order to make these topological (scale-free) ideas more quantitative, one can discuss the changes in dispersive slope and energy discontinuity δE at Θ_D that occur when the dopant density x increases above the critical density x_c (=0.06 in LSCO) towards the optimal density x_0 (=0.16 in LSCO). Fermi liquid or Landau theory says that the quasiparticle inverse slope (or mass $m^*_>$) at energies $|E-E_F|>\Theta_D$ is that of the bare quasiparticle. Because of translational invariance, momentum is a good quantum number, thus $m^*_<$ for $|E-E_F|<\Theta_D$ is related to the energy discontinuity δE at Θ_D by

$$m^*_</m^*_> = 1 - \delta = 1 - \delta E/\Theta_D \text{ (Fermi liquid only)} \qquad (1)$$

A discontinuity δE is observed, and Eq. (1) is valid experimentally for the metal-insulator transition (x near x_c), where there are large (normal) isotope effects on T_c. Near optimal doping x_o, where there are only small isotope effects on T_c, one may have $\delta E \sim 0$, but $m^*_</m^*_> > 1$. Thus the basic idea of Sommerfeld-Fermi-Landau continuum (gas or liquid) theory, in which one can treat both electrons and phonons as quasiparticles that satisfy the conservation condition (1), is satisfied in cuprates near the metal-insulator transition, but it fails as we increase the filamentary density.

To understand how δ and δE are affected by self-organization in a percolative model, one must ask what happens to the electronic states as x increases above the metal-insulator threshold at $x=x_c$. Filamentary paths are formed to provide maximal dielectric screening of internal (ionic) electrical fields, and near threshold they are nearly linear, even in the presence of disorder. Thus the crystal momentum of

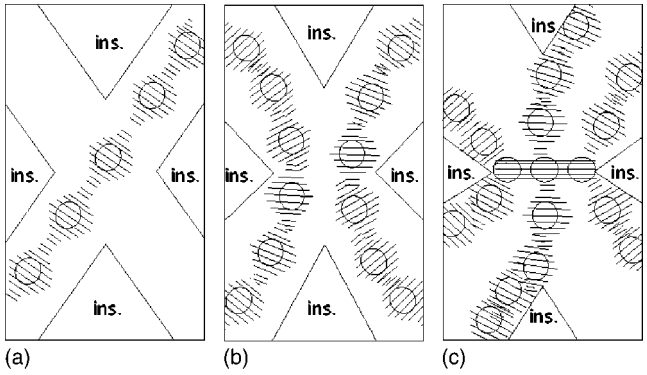

FIG. 5. A sketch of possible glassy percolative metallic paths (dashed lines), passing through dopant centers projected on the CuO_2 plane that shows how these can be crowded in overdoped samples into forming a locally liquid-metallic phase when passing through a narrow region between two insulating regions.[19,20] The regions of states resonantly bound to the circled dopants are shaded; when these regions merge, the states become locally metallic: (a) one underdoped percolative path near the insulator-metal transition, (b) near optimal doping two percolative paths can intersect and form knots that generate quasiparticle "knot" resonances at $2\Theta_D$ (Fig. 4), and (c) three percolative paths (overdoped); their intersection forms a Fermi liquid.

wave packets traveling along these nearly linear filamentary paths is well defined. As the density of filamentary paths increases, they become more and more crowded. Geometrically to avoid collisions the paths become ragged, and crystal momentum is no longer a good quantum number. Put differently, near threshold the density of percolative states is low, and interactions between carriers on different percolative paths can be neglected. This means that crystal momentum can be conserved. Further increases in x create crowding of the Fermionic carriers on nearby percolative paths, which must avoid each other according to the exclusion principle. This crowding of the percolative network is similar to the space-filling that occurs in network glasses at the glass transition. Because of the crowding, which involves both the phonons and the Fermions due to their vibronic coupling, the discontinuity δE gradually disappears as x approaches optimal doping x_o, whereas the break in mass δ remains. (In molecular glasses similar breaks in slope of $T_g(x)$ have been observed at the boundaries of stiffness phases.[27]) In addition, in LSCO near $x=x_0$, there may even be a dispersive discontinuity at $2\Theta_D$ (Fig. 4). It is tempting to connect the $2\Theta_D$ discontinuity to the "knot" formed when two filamentary paths cross [Fig. 5(b)].

Is $\delta>0$ in overdoped samples after δE has vanished at optimal and higher dopant densities? From the preliminary ARPES data[13] it is not clear whether or not (1) still holds, but even if a suitable generalization can be found, the nature of overdoped percolative paths for $|E-E_F|>\Theta_D$ is expected to be different from that for $|E-E_F|<\Theta_D$. For $x>x_o$, the cost in filamentary localization or transverse kinetic energy begins to exceed the binding energy gained from localization, especially in narrow saddle-point regions, which begin to undergo phase transitions to a Fermi liquid due to three-path intersections [Fig. 5(c)]. This effect should be larger for the more energetic states in the higher energy range $|E-E_F|>\Theta_D$; in effect, these "hot" glassy states begin to "melt" before the less energetic "cold" states with $|E-E_F|<\Theta_D$. All the less energetic states with $|E-E_F|<\Theta_D$ are constrained and glassy, but the more energetic unconstrained states with $|E-E_F|>\Theta_D$ will have larger $m^*_>$ because of this melting effect, which is characteristic of a Fermi system. Classical molecular network glasses exhibit a similar effect identified in numerical simulations with "floppy" (or cyclical) modes,[46] so it seems that the change δ in m^* at Θ_D might occur in percolative models without a discontinuity δE. However, since the anisotropy of the isotope shifts near optimal doping is proportional to the superconductive energy gap, which, in turn, is proportional to $|\cos 2\phi|$, it would seem that a broadened discontinuity δ is more consistent.

The differences between the clamping of m^* below and above Θ_D are summarized in Table I, where the predictions of constraint theory are seen to be in excellent agreement with experiment. Although these glassy results are qualitatively different from those predicted by Fermi-liquid theory or Hubbard lattice gases, quasiparticle ideas are so intuitive that more discussion is appropriate on the dispersive behavior above Θ_D, which appears to be linear (constant $m^*_>$). Because $\Theta_D=0.07$ eV$\ll$ the band width $W\sim 2$ eV, we expect that below Θ_D, $m^*_<$ should be nearly constant. However, above Θ_D it might seem from phase-space considerations that $m^*_>$ should progressively soften (decrease) as $|E-E_F|$ increases towards W. On this question the data with the least scatter are the BSCCO isotope data.[5] Most of the (^{16}O, ^{18}O) curves in their Figs. 1(b) and 2(a) show a constant $m^*_>$ up to 0.3 eV ($\sim 4\Theta_D$). However, if one looks closely at the ^{16}O nodal data[5] (virgin sample) in Fig. 2(a), curve 1, one notes something striking: unlike the other curves, where $m^*_>$ is constant for both ^{16}O and ^{18}O, here there is noticeable softening for ^{16}O, but not ^{18}O. If one is optimistic, one can actually discern in the ^{16}O curve three regions of constant $m^*_>$, with breaks at Θ_D, $2\Theta_D$, and $3\Theta_D$! These are the LO phonon harmonics, also observed (but identified only by theory)[34] in BSCCO infrared data.[33] Semiconductor luminescence spectra often exhibit LO phonon sidebands, and their observation in the Drude infrared spectra and in the ARPES dispersive spectra provides very strong support for the dopant-centered filamentary glass model.

One may wonder why the LO harmonics are observed only in that one ARPES case. Because the final excited ARPES state involves an electron with 20+ eV kinetic energy, the ARPES harmonics are weak compared to the Drude ones and are easily obscured by interactions of filamentary paths with other structural features, such as charge-density waves in the antinodal directions,[20] or built-in host strain memory effects in the isotope-exchanged ^{18}O samples. The fact that they are observed at all in the most favorable virgin ^{16}O case testifies to the remarkable quality of these ARPES data. Of course, the observation of LO phonon sidebands completely excludes alternative explanations of either the Drude or the ARPES fine structure in terms of magnons.

VI. ABSORPTIVE KINK

There is a different kind of kink at 100 meV in (Pb-doped)BSCCO, in the *width* of the ARPES peak (related to the quasiparticle scattering rate).[47] The kink appears to shift to ~70 meV in optimally doped BSCCO. This kink in the width of the photoemission peak has a perfectly conventional and straightforward explanation in terms of a distribution of charge-density wave (CDW) energy gaps with a maximum cutoff of 100 meV that is temperature independent up to ~150 K. Other work[20] chose 60 meV as the optimal energy for separating superconductive gaps and CDW gaps spatially, but the difference between these two values is small compared to their difference with 100 meV. Moreover, because of the projection of spatial inhomogeneities onto $\boldsymbol{k}$ involved in ARPES, perfect agreement is not expected. The width anomaly at 100 meV in (Pb-doped)BSCCO was explained in terms of magnon excitations, but the oscillator strength for magnon excitations should be small compared to that for CDW. The shift from 70 meV in BSCCO to 100 meV in (Pb-doped)BSCCO is also more easily explained as a pinning of CDW (with an increase in the CDW gap), than as a change in the magnon gap in the CuO_2 plane.

VII. UNIVERSALITY OF $m^*_<$ AND Θ_D: ANOTHER "MIRACLE"?

The report[14] of a nearly ideal quasiparticle discontinuity at Θ_D at threshold doping in LSCO described the observation as a "miracle." The value of $m^*_<$ observed in five different cuprates over a wide range of doping *below* Θ_D is nearly constant, much like the nanodomain diameters.[16] The actual phonon cutoffs in the host spectra measured by neutron scattering are not constant, therefore, the contrary dopant behavior is, if not a miracle, at least a major puzzle. Moreover, $m^*_>$ increases rapidly with increasing doping right through the metal-insulator transition toward large doping. We again see here an abrupt separation of the observed dispersion curves into two subsets, one constrained to be constant and independent of doping, whereas the other shows a dramatic chemical trend. Clearly this extreme behavior suggests exactly intact or broken constraints, with no intermediate cases, in other words, well-defined constraints; such well-defined subsets explain many properties of network glasses.[6,41–43] It is just this absence of partially broken constraints that distinguishes glasses in their intermediate phases from supercooled liquids. In this case the carriers are either in or out of phase with the local LO filamentary phonon.

Constraint theory explains several remarkable features of the crystal chemistry of the cuprates. A general characteristic of all perovskite and pseudoperovskite oxides is that they are subject to a very wide variety of lattice instabilities, generally taken to be an indication of attractive strong electron-phonon interactions. Lattice instabilities are commonly observed in metallic alloys and are often the factor that limits T_c, as the lattices stabilize themselves through deformations that lower the total energy and reduce these interactions.[45] However, there are many instabilities in transition-metal oxides, yet most of them are not dopable, and although the nondopable manganites can be rendered metallic by alloying, they cannot be made superconductive. The origin of this behavior is the global instability of cuprate networks, viewed as nearly glassy and underconstrained.[40] At low temperatures such networks should undergo Jahn-Teller distortions to become insulating.

According to constraint theory, one of the factors that enables the cuprates to avoid unfavorable distortions is that the CuO_2 planes are isostatic (rigid but unstressed), whereas all the other planes are underconstrained (soft and locally buckled).[40] This means that near dopants, located in the planes adjacent to CuO_2 planes or in other metallic planes, $\boldsymbol{k}$ is no longer a good quantum number, and only the phonon and electron states in CuO_2 planes show up in ARPES data as resolvable peaks. Moreover, the residual impact of softening associated with unconstrained relaxation in the dopant-deformed underconstrained planes applies only to $m^*_>$ above Θ_D, accounting for the monotonic increase of $m^*_>$ as electron-phonon interactions are screened with increasing dopant concentration. It should be stressed that this dynamical dopant screening effect is not the result of magnon exchange, as is made abundantly clear by the isotopic dependence of $m^*_>$ in the BSCCO experiments,[5] which extends to high energies far outside the magnon range. Note also that dynamical dopant screening above Θ_D has little effect on T_c, as the high-energy repulsive interactions above Θ_D add only a logarithmic correction λc of order 0.2 to the superconductive coupling constant $\lambda^* = \lambda - \lambda_C$, which depends mainly on the strength of the attractive electron-phonon interactions λ *below* Θ_D.

At $x = 0.03$, below the metal-insulator transition in $La_{2-x}Sr_xCuO_4$ at $x = x_c = 0.063$, the discontinuity δ is even larger and narrower[13] than at $x = x_c$. What does this mean? It means that even at this low doping level the dopants are forming line segments to maximize their conductivity and the associated dielectric screening energy. The segments are too short to produce a metal-insulator transition at low energies, but at photon energies ~20 eV, mean-free paths are so short (~10 nm) that these line segments look linear, with negligible intersegment scattering.

VIII. CONCLUSIONS

We have shown that discrete *glassy* percolative constraint theory[6,40–43] successfully explains all the major features of the recent photoemission[5,13,14] and STM[19,20] data without introducing new axioms. The most conspicuous features are the *rigidity* of the subLO phonon states and the variable *softness* of superLO phonon states. The explanation for this anomalous electromechanical behavior in a glassy context relies heavily on analogies with the strikingly similar mechanical behavior of network glasses. The latter has been well studied experimentally and simulated in great numerical detail, in studies extending over the last 25 years.[43] Given the unprecedented complexity of the electromechanical behavior of the cuprates, these mechanical analogies provide further evidence of the presence of strong electron-phonon interactions in the cuprates, and indicate that these attractive interactions are the cause of HTSC, as always supposed by Mueller.[1,2]

Many strongly correlated continuum "liquid" or "glue" (polynomial) Hamiltonian models have been proposed to explain various facets of HTSC, involving magnons,[47] charge-density waves (CDWs) (everything except dopants), but rarely phonons, which are of course *necessary* to explain the observed isotope effects.[5] The nontopological (nonglassy) models *expand* the Fermi-liquid coordinate space with auxiliary spin or CDW variables. CDWs dilute attractive electron-phonon interactions by reducing $N(E_F)$, and magnetic moments break Cooper pairs. Thus auxiliary spin or CDW interactions can only *reduce* T_c and cannot explain HTSC. Auxiliary spin or CDW models met with small successes in explaining individual experiments, but no overall success, and they failed completely to explain phonon kinks and large isotope effects. Given its deep and extensive basis in experiment,[43,48] the success of glassy percolative constraint theory (which actually *contracts* the liquid coordinate space to form the frozen filamentary glass) in explaining *high* TSC should not be surprising, but the origin of its successful prediction of the rigidity of sub-LO phonon dispersion may not be obvious. Constraints effectively *define* the glassy state and are generic to it.[43] The cuprates are simply well-studied electronic glasses with very strong electron-phonon interactions, in which constraint-imposed rigidity has been observed spectroscopically.

Constraint theory is an axiomatic hierarchical theory that treats (long-range) strain effects on self-organized networks in strongly disordered glassy solids (both molecular and electronic); it is supported by many successful studies that depend on the short-range character of covalent bonding forces.[43] Coulomb interactions are present in the cuprates in addition to short-range interatomic forces, but these seem to affect HTSC only indirectly (mainly through enhancing electron-phonon interactions by resonantly binding carriers to soft dopants). This is not surprising, as attractive electron-phonon energies are short range and must be dominant in order to achieve high T_c's. Thus it is also not surprising that no new axioms have been introduced here to explain the ARPES and STM data.

The successes of constraint theory span a wide range of combinatorially "insoluble" (exponentially difficult) problems, including even the nature and structure of proteins in their transition states.[43,49] The success reported here is unforced; in connection with the protein successes, one is justified in saying that cuprate HTSC are "almost alive." The self-organized nature of the configurationally glassy electronic network explains the anomalous cancellation (rigidity) effects in $m^*_<$ below Θ_D, as well as the seemingly uncontrolled, strongly dopant-dependent isotope effects in $m^*_>$ above Θ_D. The latter surely reflect the marginal mechanical instability of these pseudoperovskite lattices.[40] One can conjecture that the success of the hierarchical theory of electronic rigidity in HTSC stems primarily from the long-range nature of both Coulomb and strain interactions, which generate a narrow band of dopant-centered filamentary states pinned to E_F.

Although the anomalous rigidity of states within a Debye energy of the Fermi energy is a natural consequence of the topological glass model, one may reasonably ask which features of the data are not explicable topologically. An example is the magnitudes a, b, and $c(x)$ of the large isotope and dopant concentration dependence of $m^*_>$ discussed above and in Table I. Although the theory of marginal elastic stability explains why $c'(x)$ is so large, it does not explain the magnitude quantitatively. To do so would apparently require a first-principles calculation of the anisotropic relaxation (strain) field around dopant strings, which thus far lies well outside the range of the state of the computational art, as applied, for example,[50] to MgB_2 (six atoms/cell). Such a calculation would involve at least as many atoms as are found in a nanodomain ($\sim 10^3$), with the dopants arranged to minimize the energy by forming filaments. Problems of this kind in the cuprates are unavoidably better treated topologically than by brute force.

Another interesting problem is the origin of the dispersive kink at $2\Theta_D$ that may have been observed in LSCO at optimal doping (Fig. 4). Here it has been suggested that this kink might arise from "knots" formed by intersections of two dopant-centered paths in narrow bottlenecks of a nanodomain landscape [Fig. 5(b)]. It is noteworthy that a dispersive kink at $2\Theta_D$ has thus far not been observed in BSCCO. A possible topological explanation for this is that although there is only one metallic CuO_2 plane in LSCO, there are two metallic BiO_2 and CuO_2 planes in BSCCO, so that two paths can avoid each other by using alternating planes. It will be interesting to see if this difference survives in future experiments. If it does, it will then be even more interesting to see if this difference between BSCCO and LSCO can be explained by more conventional (nonglassy) theories.

The possibility that oxide percolative paths can be self-organized may not be restricted to cuprates. Thin films of *a*-(In, Ga, Zn)O are apparently filamentary metals at carrier concentrations as low as 10^{16}/cc, whereas single-crystalline $InGaO_3(ZnO)_5$ is metallic only for carrier densities above 10^{18}/cc. For these materials a natural path to flexible self-organization would involve In enrichment of the strings illustrated in their Fig. 1. Because these materials are stiff mechanically, in them electron-phonon interactions are too weak to produce superconductivity, but these transparent films are technologically promising filamentary metals.[51]

Various interpretations of cuprate resistivity data $\rho(T)$ are reviewed recently, and it is suggested that $d^2\rho/dT^2$ can be used to construct electronic phase diagrams.[52] The discussion of these diagrams is essentially phenomenological, because it is difficult to construct quantitative theoretical models for $\rho(T)$. The most noteworthy feature of the diagrams is the unexplained *linearity* of the white "zero curvature" critical regions ρ_c (marked with a dashed line in their Fig. 2 for LSCO, for example) *over wide ranges of composition and temperature*; this is characteristic of a topological or percolative, not analytic or algebraic, property. There is a simple explanation for this linearity of ρ_c: it is the result of the linearity of the number of percolation paths with site-occupation probability p, known from many numerical simulations.[46] Strict resistivity linearity, $d^2\rho/dT^2=0$, at high T is generally observed only at or very near optimal doping (nearly vertical white lines ρ_c in Figs. 1 and 2 of Ref. 46 BSLCO and LSCO). At optimal doping the filling factor for

the filamentary intermediate phase is maximized,[53] whereas the filling factors for the neighboring nonpercolative insulating and normal metallic phases are nearly zero.

Several thousand papers have discussed HTSC in the context of a single-phase (mean-field) Hubbard model. The mean-field Hubbard contact-interaction model predicts no phonon effects on the electronic spectrum near the Fermi energy;[54] this result is included in Table I. Whether or not it represents an improvement on Fermi liquid theory may be a matter of taste. Finally, the importance of electron-phonon interactions in the theory of HTSC is emphasized in a recent summary.[55]

[1] J. G. Bednorz and K. A. Mueller, Z. Phys. B: Condens. Matter **64**, 189 (1986).
[2] K. A. Mueller, Physica C **341**, 11 (2000).
[3] J. C. Phillips, Phys. Rev. B **36**, 861 (1987); Phys. Rev. B **43**, 6257 (1991).
[4] J. C. Phillips, Philos. Mag. B **81**, 757 (2001).
[5] G.-H. Gweon, T. Sasagawa, S. Y. Zhou, J. Graf, H. Takagi, and A. Lanzara, Nature (London) **430**, 187 (2004).
[6] J. C. Phillips, Phys. Rev. Lett. **88**, 216401 (2002).
[7] A. Lanzara *et al.*, Nature (London) **412**, 510 (2001).
[8] R. J. McQueeney, J. L. Sarrao, P. G. Pagliuso, P. W. Stephens, and R. Osborn, Phys. Rev. Lett. **87**, 077001 (2001).
[9] R. J. McQueeney, Y. Petrov, T. Egami, M. Yethiraj, G. Shirane, and Y. Endoh, Phys. Rev. Lett. **82**, 628 (1999).
[10] S. Engelsberg and J. R. Schrieffer, Phys. Rev. **131**, 993 (1963).
[11] D. M. Tang, J. Li, and C.-D. Gong, Phys. Rev. B **67**, 235421 (2003).
[12] J. C. Phillips, *Physics of High-T_c Superconductivity* (Academic, Boston, 1989).
[13] X. J. Zhou *et al.*, Nature (London) **423**, 398 (2003).
[14] X. J. Zhou *et al.*, Phys. Rev. Lett. **92**, 187001 (2004).
[15] S. H. Pan *et al.*, Nature (London) **413**, 282 (2001).
[16] K. M. Lang, V. Madhavan, J. E. Hoffman, E. W. Hudson, H. Eisaki, S. Uchida, and J. C. Davis, Nature (London) **415**, 412 (2002).
[17] J. C. Phillips, Philos. Mag. B **79**, 1477 (1997).
[18] J. C. Phillips, Philos. Mag. B **83**, 3267 (2003).
[19] K. McElroy, R. W. Simmonds, D.-H. Lee, J. Orenstein, H. Eisaki, S. Uchida, and J. C. Davis, Nature (London) **422**, 592 (2003).
[20] K. McElroy, D.-H. Lee, J. E. Hoffman, K. M. Lang, E. W. Hudson, H. Eisaki, S. Uchida, J. Lee, and J. C. Davis, cond-mat/0404005 (unpublished).
[21] M. Lee, G. S. Jeon, and M. Y. Choi, Phys. Rev. B **66**, 075304 (2002).
[22] J. C. Phillips, Philos. Mag. B **83**, 3255, (2004).
[23] J. C. Phillips, Phys. Rev. B **41**, 8968 (1990).
[24] J. C. Phillips, Solid State Commun. **109**, 301 (1999).
[25] J. C. Phillips, Phys. Rev. B **47**, 11 615 (1993).
[26] C. C. Homes, S. V. Dordevic, M. Strongin, D. A. Bonn, R. X. Liang, W. N. Hardy, S. Komiya, Y. Ando, G. Yu, N. Kaneko, X. Zhao, M. Greven, D. N. Basov, and T. Timusk, Nature (London) **430**, 539 (2004).
[27] Y. Wang, J. Wells, D. G. Georgiev, P. Boolchand, K. Jackson, and M. Micoulaut, Phys. Rev. Lett. **87**, 185503 (2001).
[28] M. F. Thorpe, M. V. Chubinsky, D. J. Jacobs, and J. C. Phillips, J. Non-Cryst. Solids **266-269**, 859 (2000).
[29] M. Micoulaut and J. C. Phillips, Phys. Rev. B **67**, 104204 (2003).
[30] J. Barre, A. R. Bishop, T. Lookman, and A. Saxena, cond-mat/0408385 (unpublished).
[31] A. Lucarelli *et al.*, Phys. Rev. Lett. **90**, 037002 (2003).
[32] M. Ortolani, V. Morano P. Calvani, P. Maselli, L. Maritato, M. Fujita, K. Yamada, and M. Colapietro, J. Supercond. **17**, 127 (2004).
[33] J. Hwang, T. Timusk, and G. D. Gu, Nature (London) **427**, 714 (2004).
[34] J. C. Phillips, Phys. Status Solidi B **242**, 51 (2005).
[35] J. C. Phillips and J. Jung, Philos. Mag. B **82**, 1163 (2002).
[36] M. L. Kulic and O. V. Dolgov, cond-mat/0405540 (unpublished).
[37] M. Abrecht, D. Ariosa, D. Cloetta, S. Mitrovic, M. Onellion, X. X. Xi, G. Margaritondo, and D. Pavuna, Phys. Rev. Lett. **91**, 057002 (2003).
[38] H. J. Choi, M. L. Cohen, and S. G. Louie, Physica C **385**, 66 (2003).
[39] G. Lucovsky and J. C. Phillips, Appl. Phys. A: Mater. Sci. Process. **78**, 453 (2004); J. Vac. Sci. Technol. B **22**, 2087 (2004).
[40] J. C. Phillips, Philos. Mag. B **85**, 931 (2005).
[41] J. C. Phillips, J. Non-Cryst. Solids **34**, 153 (1979).
[42] J. C. Phillips, Phys. Today **35**(2), 27 (1982).
[43] P. Boolchand, G. Lucovsky, J. C. Phillips, and M. F. Thorpe, cond-mat/0502312 (unpublished).
[44] H. D. Sun, Y. Segawa, M. Kawasaki, A. Ohtomo, K. Tamura, and H. Koinuma, J. Appl. Phys. **91**, 6457 (2002).
[45] J. C. Phillips, *Physics of High-T_c Superconductivity* (Academic, Boston, 1989).
[46] H. He and M. F. Thorpe, Phys. Rev. Lett. **54**, 2107 (1985).
[47] A. A. Kordyuk *et al.*, Phys. Rev. Lett. **92**, 257006 (2004).
[48] J. C. Phillips, A. Saxena, and A. R. Bishop, Rep. Prog. Phys. **66**, 2111 (2003).
[49] A. J. Rader, B. M. Hespenheide, L. A. Kuhn, and M. F. Thorpe, Proc. Natl. Acad. Sci. U.S.A. **99**, 3540 (2002).
[50] A. Floris, G. Profeta, N. N. Lathiotakis, M. Luders, M. A. L. Marques, C. Franchini, E. K. U. Gross, A. Continenza, and S. Massidda, Phys. Rev. Lett. **94**, 037004 (2005).
[51] K. Nomura, H. Ohta, A. Takagi, T. Kamiya, M. Hirano, and H. Hosono, Nature (London) **432**, 488 (2004).
[52] Y. Ando, S. Komiya, K. Segawa, S. Ono, and Y. Kurita, Phys. Rev. Lett. **93**, 267001 (2004).
[53] J. C. Phillips, Philos. Mag. B **83**, 1949 (2004).
[54] G. Sangiovanni, M. Capone, C. Castellani, and M. Grilli, Phys. Rev. Lett. **94**, 026401 (2005).
[55] V. L. Ginzburg and E. G. Maksimov, Phys. Status Solidi B **242**, 9 (2005).